negative selection is increased. This results in an A2-restricted repertoire that contains receptors with higher than usual affinity for A2 per se. When provided with the A2/K^b molecule, murine CD8 can participate more fully in interaction with the restriction element, thus elevating the avidity of the interaction above the threshold required for the induction of detectable lytic activity in the absence of antigen. However, because CD8 is also required for T cell stimulation, our results are also consistent with a model in which only the affinity cutoff for negative selection is increased and the observed recognition of A2 per se is due to an increase in the affinity requirement for antigen responsiveness rather than positive selection.

REFERENCES AND NOTES

1. M. M. Davis and P. J. Bjorkman, *Nature* **334**, 395 (1988).
2. R. D. Salter *et al.*, *ibid.* **345**, 41 (1990).
3. J. M. Connolly, T. A. Potter, E.-M. Wormstall, T. H. Hansen, *J. Exp. Med.* **168**, 325 (1988); T. A. Potter, T. V. Rajan, R. F. Dick II, J. A. Bluestone, *Nature* **337**, 73 (1989).
4. M. J. Bevan, *Nature* **269**, 417 (1977); R. M. Zinkernagel *et al.*, *J. Exp. Med.* **147**, 882 (1978); W. C. Sha *et al.*, *Nature* **335**, 271 (1988); H. S. Teh *et al.*, *ibid.*, p. 229; P. Kisielow, H. S. Teh, H. Bluthmann, H. von Boehmer, *ibid.*, p. 730; L. J. Berg *et al.*, *Cell* **58**, 1035 (1989); J. Kaye *et al.*, *Nature* **341**, 746 (1989); W. C. Sha *et al.*, *Proc. Natl. Acad. Sci. U.S.A.* **87**, 6186 (1990).
5. J. W. Kappler, N. Roehm, P. Marrack, *Cell* **49**, 273 (1987); J. W. Kappler, U. Staerz, J. White, P. Marrack, *Nature* **332**, 35 (1988); H. R. MacDonald *et al.*, *ibid.*, p. 40; W. C. Sha *et al.*, *ibid.* **336**, 73; H. S. Teh, H. Kishi, B. Scott, H. von Boehmer, *J. Exp. Med.* **169**, 795 (1989).
6. N. A. Lee, D. Y. Loh, E. Lacy, *J. Exp. Med.* **175**, 1013 (1992); M. Blum *et al.*, *Cell* **69**, 1097 (1992).
7. R. C. Duke, *J. Exp. Med.* **170**, 59 (1989).
8. M. J. Irwin, W. R. Heath, L. A. Sherman, *ibid.*, p. 1091.
9. N. L. Samberg, E. C. Scarlett, H. J. Strauss, *Eur. J. Immunol.* **19**, 2349 (1989).
10. U. Kalinke, B. Arnold, G. J. Hammerling, *Nature* **348**, 642 (1990).
11. A. Vitiello, D. Marchesini, J. Furze, L. A. Sherman, R. W. Chestnut, *J. Exp. Med.* **173**, 1007 (1991).
12. F. H. Gotch *et al.*, *Nature* **326**, 881 (1987).
13. V. H. Engelhard, E. Lacy, J. P. Ridge, *J. Immunol.* **146**, 1226 (1991).
14. D. La Face *et al.*, *FASEB J.* **6** (Abstr. 4474), A1709 (1992).
15. A. L. Ingold, C. Landel, C. Knall, G. A. Evans, T. A. Potter, *Nature* **352**, 721 (1991); C. J. Aldrich *et al.*, *ibid.*, p. 718.
16. B. H. Koller and H. T. Orr, *J. Immunol.* **134**, 2727 (1985).
17. A. Vitiello and L. A. Sherman, *ibid.* **131**, 1635 (1983).

18. We thank J. Price for assistance in production of transgenic mice and C. Wood for excellent secretarial assistance. Supported by grant CA 25803 from the National Cancer Institute of the National Institutes of Health.

9 July 1992; accepted 23 September 1992

Comparative Genomic Hybridization for Molecular Cytogenetic Analysis of Solid Tumors

Anne Kallioniemi,* Olli-P. Kallioniemi, Damir Sudar, Denis Rutovitz, Joe W. Gray, Fred Waldman, Dan Pinkel

Comparative genomic hybridization produces a map of DNA sequence copy number as a function of chromosomal location throughout the entire genome. Differentially labeled test DNA and normal reference DNA are hybridized simultaneously to normal chromosome spreads. The hybridization is detected with two different fluorochromes. Regions of gain or loss of DNA sequences, such as deletions, duplications, or amplifications, are seen as changes in the ratio of the intensities of the two fluorochromes along the target chromosomes. Analysis of tumor cell lines and primary bladder tumors identified 16 different regions of amplification, many in loci not previously known to be amplified.

The discovery of genetic changes involved in the development of solid tumors has proven difficult. Karyotyping is impeded by the low number of high-quality metaphase spreads and the complex nature of chromosomal changes (*1*). Molecular genetic studies of isolated tumor DNA have been more successful and have been used to detect common regions of allelic loss, mutation, or amplification (*2*, *3*). However, such molecular methods are highly focused; they target one specific gene or chromosome region at a time and leave the majority of the genome unexamined.

We have developed a molecular cytogenetic method, comparative genomic hybridization (CGH), that is capable of detecting and mapping relative DNA sequence copy number between genomes. A copy number karyotype can be generated for a tumor by the comparison of DNAs from malignant and normal cells, thereby identifying regions of gain or loss of DNA. In this application of CGH, biotinylated total tumor DNA and digoxigenin-labeled normal genomic reference DNA are simultaneously hybridized to normal metaphase spreads in the presence of unlabeled Cot-1 blocking DNA (*4*). Hybridization of tumor DNA is detected with green-fluorescing fluorescein isothiocyanate (FITC)–avidin, and the reference DNA hybridization is detected with red-fluorescing rhodamine antidigoxigenin (*5*). The relative amounts of tumor and reference DNA bound at a given chromosomal locus are dependent on the relative abundance of those sequences in the two DNA samples and can be quantitated by measurement of the ratio of green-to-red fluorescence. The reference DNA serves as a control for local variations in the ability to hybridize to target chromosomes. Thus, gene amplification or chromosomal duplication in the tumor DNA produces an elevated green-to-red ratio, and deletions or chromosomal loss cause a reduced ratio. The Cot-1 DNA included in the hybridization inhibits binding of the labeled DNA to the centromeric and heterochromatic regions, so these regions are excluded from the analysis. The fluorescence signals are quantitatively analyzed by means of a digital image analysis system (*6*). A software program integrates the green and red fluorescence intensities in strips orthogonal to the chromosomal axis, subtracts local background, and calculates intensity profiles for both colors and the green-to-red ratio along each chromosome.

The ability of CGH to quantitate changes in sequence copy number that affect an entire chromosome was tested with five fibroblast cell lines having one to five copies of the X chromosome and two copies of each autosome (*7*). Hybridization of DNA from a 45,X0 cell line (in green), together with normal female reference DNA (in red) to a normal male metaphase spread, resulted in a uniform green-red staining of the autosomes, whereas the X chromosome appeared more red (Fig. 1A). Hybridizations with DNA from cell lines carrying two, three, four, or five copies of the X chromosome resulted in increasingly strong green fluorescence from the X chromosome relative to the autosomes. The average green-to-red fluorescence ratio of the X chromosome (Fig. 1B), when normalized to the average ratio for the autosomes within the same metaphase spread, increased linearly with increasing number of X chromosomes [correlation coefficient (r) = 0.978]. Thus, CGH can quantitatively distinguish a change of plus or minus one copy of a chromosome at least up to four copies.

We used CGH to generate a complete copy number karyotype for a near-diploid breast cancer cell line, 600PE. According to the published karyotype (*8*), 600PE is near-diploid with five marker chromo-

A. Kallioniemi, O.-P. Kallioniemi, D. Sudar, J. W. Gray, F. Waldman, D. Pinkel, Division of Molecular Cytometry, Department of Laboratory Medicine, University of California at San Francisco, San Francisco, CA 94143. D. Rutovitz, Medical Research Council Human Genetics Unit, Western General Hospital, Edinburgh EH4 2XU, United Kingdom.

*To whom correspondence should be addressed.

somes. The CGH with biotinylated 600PE DNA (in green) and normal digoxigenin-labeled reference DNA (in red) revealed the following relative copy number changes: gain of 1q and loss of 9p, 16q, 17p, and distal 11q. The green-to-red ratio profiles for these aberrant chromosomes are shown in Fig. 2. Fluorescence in situ hybridization (FISH) with locus-specific 16p and 16q cosmid probes to 600PE cells (9) found two signals per nucleus for 16p and one for 16q that permitted calibration of a green-to-red ratio of 1.0 as indicating two copies of a sequence.

Thus, if the absolute copy number of any region in a tumor genome is known, relative numbers can be converted to actual copy numbers at all loci. The CGH results differed from the originally published karyotype in the region of 16p and proximal 1p. This discrepancy was subsequently resolved based on the FISH analysis with locus-specific probes that indicated that the components of one of the marker chromosomes had been misinterpreted by conventional cytogenetic analysis (8). CGH with DNA from two fibroblast cell lines (*10*) detected small interstitial deletions around the *RB1* locus: del (13) (pter>q14.1::q21.2>qter) and del (13) (pter>q14.1::q22.1>qter). On the basis of the CGH analysis and measurement of the deletion size as a fraction of the length of chromosome 13 (total length 111 Mb), these deletions were estimated to span about 10 and 20 Mb, respectively. Thus, it is possible that CGH could be used to screen DNA samples from solid tumors in order to identify physical deletions that may uncover recessive mutant tumor suppressor genes.

The CGH technique was evaluated for its ability to detect increased gene copy number with cell lines that contained previously reported amplification of oncogenes. CGH was performed with DNA from a colon cancer cell line, COLO 320HSR (Fig. 3A), known to contain more than a 50-fold amplification of a 300-kb region around the *myc* oncogene (*11*). The expected high green-to-red ratio at 8q24 that corresponds to the *myc* locus is clear. The height of the peak does not quantitatively reflect the level of amplification because the fluorescent signal spreads over a region of the chromosome that is larger than the length of the amplicon. This is apparently a result of the complex organization of the target DNA in the denatured

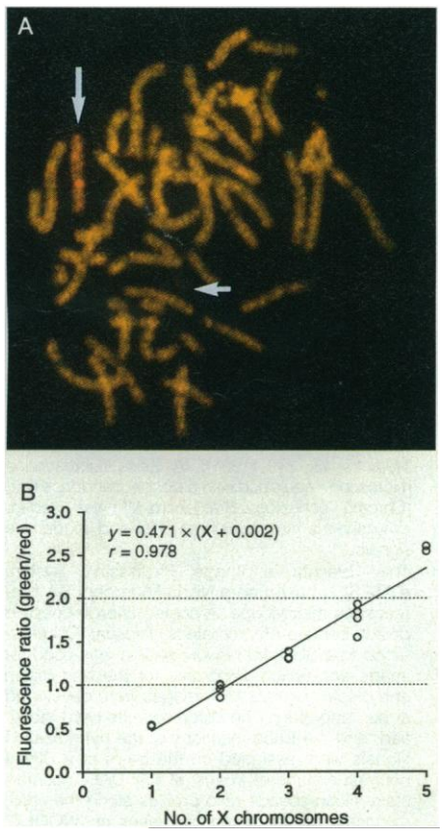

Fig. 1. (**A**) Hybridization of DNA from the 45,X0 cell line (green) and normal female reference DNA (red) to a normal male metaphase spread. The reddish color of the X chromosome (large arrow) as compared with autosomes reflects the lower relative copy number of the X chromosome sequences in this cell line. Faint staining of a small part of the Y chromosome (small arrow) is a result of the homologous sequences in the pseudo-autosomal region. (**B**) Correlation of the number of X chromosomes in five fibroblast cell lines and the average green-to-red ratio of the X chromosome relative to the same ratio for the autosomes.

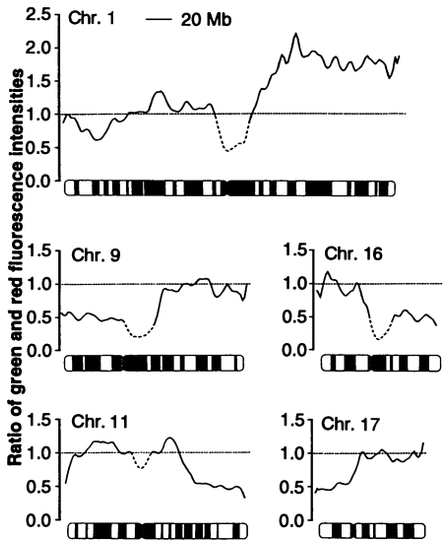

Fig. 2. Green-to-red fluorescence ratio profiles of chromosomes 1, 9, 11, 16, and 17 after hybridization with 600PE DNA (green) and normal reference DNA (red). Profiles reflect the relative copy number of the chromosomal regions. FISH of 600PE interphase and metaphase cells indicated that the copy number for 16p loci was 2. Thus, the ratio of 1.0 indicates two copies of the sequence throughout the genome. The dip in the profile at 1p34 through 1p36 may represent a previously unsuspected small interstitial deletion but has not been verified independently with specific probes for this region. Centromeric and heterochromatic regions of the genome are not included in the analysis because the Cot-1 DNA partially blocks signals in these regions, and the large copy number polymorphisms between individuals at these loci make the ratio data unreliable. Chr., chromosome.

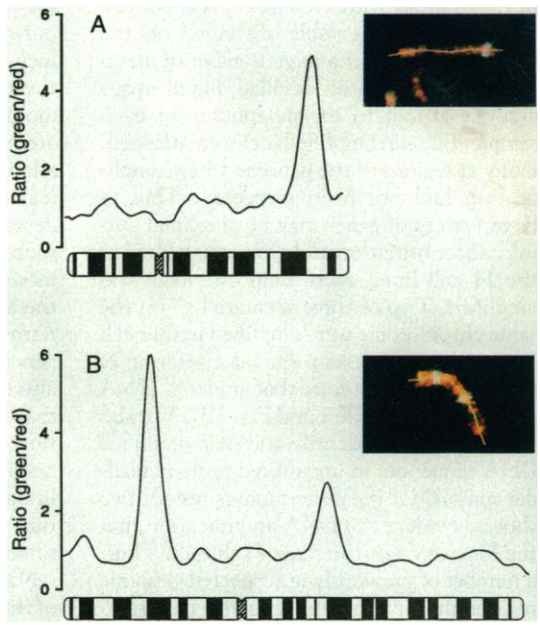

Fig. 3. Green-to-red fluorescence ratio profiles of chromosome 8 (**A**) and chromosome 2 (**B**) after hybridization with COLO 320HSR and NCI-H69 cell line DNAs, respectively (green). Normal reference DNA included in the hybridization is shown in red. The inserts show the overlaid green and red fluorescence images of the chromosomes and the chromosomal medial axis drawn by the image analysis program. In (A), the *myc* locus at 8q24 shows a highly elevated green-to-red ratio, which is compatible with the known high-level amplification of *myc* in the COLO 320HSR cell line. In (B), three regions of amplification are seen on chromosome 2. The signal at 2p24 corresponds to the location of N-*myc* known to be amplified in the NCI-H69 cell line. The two other regions with a highly increased fluorescence ratio, at 2p21 and 2q21, were not known to be amplified.

Table 1. Mapping of amplified sequences in established cancer cell lines and primary tumors by CGH. Cytogenetic information is based on the American Type Culture Collection catalog of cell lines and hybridomas (1992). DM, double minute chromosomes; HSR, homogeneously staining regions.

Specimen	Origin	Amplification by CGH*	Cytogenetic evidence of gene amplification
		Cell lines	
5637	Bladder	3p25, 6p22	DM
SK-BR-3	Breast	8q24 (*myc*), 8q21, 17q12 (*erb*B2), 20q13	—
COLO 205	Colorectal	6p21, 6q24	—
NCI-H508	Colorectal	14q12-q13	DM
SW480	Colorectal	8q24 (*myc*)	DM
SW620	Colorectal	16q21-q23	HSR
WiDr	Colorectal	8q23-q24 (*myc*)	—
SK-N-MC	Neuroblastoma	8q24 (*myc*)	DM
Calu-3	Small cell lung	8p12-p21, 8qtel, 17q12 (*erb*B2)	HSR
Calu-6	Small cell lung	13q32-q34	—
NCI-H69	Small cell lung	2p24 (N-*myc*), 2p21, 2q21	—
		Primary tumors	
UR140	Bladder carcinoma	16q21-q22	—
UR145	Bladder carcinoma	6p22	—

*The oncogene most likely involved in this amplification is shown in parentheses.

chromosomes. The eightfold amplification of the *erbB2* oncogene in the SK-BR-3 breast cancer cell line also was detectable as a hybridization signal at 17q12 (Table 1) with CGH. High-level amplifications such as these could also be detected in single-color hybridizations with the use of only labeled tumor DNA.

Cytogenetic and molecular studies of primary tumors and cell lines often reveal homogeneously staining regions and double minute chromosomes that do not involve known oncogenes (*12*). The CGH technique provides a means to detect and map such sequences. Table 1 contains a summary of the analysis with CGH of 11 cancer cell lines. Data in the table are based on the visual inspection of a large number of metaphase spreads and on detailed digital image analysis of four to six metaphases for each sample. Sixteen amplified loci were mapped, many at regions of the genome where amplification had not been suspected. Thus, a large variety of genes may be amplified during cancer initiation and progression. In 5 of the 11 cell lines, more than one locus was amplified. Two or three separate loci on the same chromosome were amplified in four cell lines, which suggests a spatial clustering of chromosomal locations that undergo DNA amplification (Table 1 and Fig. 3B). We also applied CGH to identify and map amplified DNA sequences in uncultured primary bladder tumors. Of the seven tumors tested, two showed evidence of DNA amplification, but the loci were not the same (Table 1). Thus, a number of previously unsuspected genomic regions that might contain genes important for cancer progression have been identified. Further studies will be required to determine which loci contain novel oncogenes and which represent coincidental, random DNA amplification characteristic of general genomic instability.

The detection and mapping of unknown amplified sequences that typically span several hundred kilobases to a few megabases demonstrates the usefulness of the CGH technique for rapid identification of regions of the genome that may contain oncogenes. Similarly, detection of deletions may facilitate identification of regions that contain tumor suppressor genes. The ability to survey the whole genome in a single hybridization is a distinct advantage over allelic loss studies by restriction fragment length polymorphism (RFLP) that target only one locus at a time. RFLP is also restricted by the availability and informativeness of polymorphic probes. However, further studies are required to establish to what extent allelic losses in tumors are caused by physical deletions. In clinical specimens, the detection of small copy number differences, such as those associated with deletions, is more difficult than in cell lines because of the admixture of DNA from contaminating normal cells and because of intratumor genetic heterogeneity. Like RFLP, CGH also emphasizes the detection of aberrations that are homogeneous in the cell population and averages those that are heterogeneous. Currently, sensitivity is primarily limited by the granularity of the hybridization signals in the metaphase chromosomes. We expect further improvements in sensitivity will be achieved by optimization of the probe concentration and labeling and by the averaging of the green-to-red fluorescence ratios from several metaphase spreads. CGH comparisons other than those described here—for example, between primary tumors and their metastases—should also be informative.

REFERENCES AND NOTES

1. J. R. Teyssier, *Cancer Genet. Cytogenet.* **37**, 103 (1989).
2. E. R. Fearon and B. Vogelstein, *Cell* **61**, 759 (1990); T. Sato *et al.*, *Cancer Res.* **50**, 7184 (1990).
3. K. Alitalo and M. Schwab, *Adv. Cancer Res.* **47**, 235 (1986); M. Schwab and L. C. Amler, *Genes Chrom. Cancer* 1, 181 (1990).
4. DNAs were labeled with biotin-14–deoxyadenosine triphosphate or digoxigenin-11–deoxyuridine triphosphate by nick translation. The optimal size for double-stranded probe fragments was 600 to 1000 bp. Lymphocyte metaphase preparations were denatured in 70% formamide and 2× SSC [1× SSC is 0.15 M NaCl and 0.015 M Na citrate (pH 7)] at 70°C for 2 to 3 min and dehydrated in a sequence of 70%, 85%, and 100% ethanol. The slides were air-dried, treated with Proteinase K (0.2 μg/ml) (Boehringer Mannheim) for 7.5 min at 37°C in 20 mM tris and 2 mM $CaCl_2$ (pH 7.5), and dehydrated by ethanol as above. Sixty nanograms of biotinylated test DNA, 60 ng of digoxigenin-labeled normal reference DNA, and 5 μg of unlabeled Cot-1 DNA (BRL, Gaithersburg, MD) were precipitated with ethanol and dissolved in 10 μl of 50% formamide, 10% dextran sulfate, and 2× SSC (pH 7). This probe mixture was denatured at 70°C for 5 min, allowed to reanneal at 37°C for 60 min, and hybridized to normal male metaphase chromosomes for 3 to 4 days at 37°C.
5. Slides were washed at 45°C three times in 50% formamide–2× SSC (pH 7), twice in 2× SSC, and once in 0.1× SSC (10 min for each wash). After washing, the slides were immunocytochemically stained at room temperature in three 30-min steps: (i) FITC-avidin (5 μg/ml; Vector Laboratories, Burlingame, CA) and antidigoxigenin-rhodamine (2 μg/ml; Boehringer Mannheim); (ii) antiavidin (5 μg/ml; Vector Laboratories); and (iii) FITC-avidin (5 μg/ml). Nuclei were counter-stained with 0.8 μM 4,6-diamino-2-phenylindole (DAPI) in an antifade solution [G. D. Johnson and J. G. M. Nogueria, *J. Immunol. Methods* **43**, 349 (1981)]. A Zeiss fluorescence microscope equipped with a double bandpass filter (Chroma Technology, Brattleboro, VT) was used for simultaneous visualization of FITC and rhodamine signals.
6. The Quantitative Image Processing System (QUIPS) is based on a Nikon Microphot SA fluorescence microscope. A cooled charge-coupled device camera (Photometrics, Tucson, AZ) interfaced to a SUN 4/330 work station was used for image acquisition. Programs for the acquisition and display of multicolor images were developed at our laboratory. The chromosomes were identified, and the band locations of the hybridization signals were assigned on the basis of a digital contrast-enhanced image of the DAPI counterstain. Fluorescence ratio profiles along the chromosomes are extracted by means of "WOOLZ" software package (developed at the Medical Research Council, Edinburgh) as follows. The DAPI image is used to set the morphological boundary of each chromosome by thresholding. The chromosome outline is smoothed by an *n* number of opening and closing operations, and the medial axis of the chromosome is determined. The DAPI image is expanded outward in all directions until the intensity field levels off (when background is reached) or begins to rise (because of an adjacent chromosome). The intensity profile of each image along the medial axis and within the expanded DAPI image is then calculated by a summation of the green and red fluorescence pixel values along the sequence of lines perpendicular to and spaced at unit distance along the medial axis. Modal green and red intensity values

that correspond to the expanded DAPI image are used to represent background fluorescence and are used as the intensity origin.

7. GMO1723 (45,XO), GM08399 (46,XX), GMO4626 (47,XXX), GMO1415E (48,XXXX), and GMO5009B (49,XXXXX) from the National Institute of General Medical Sciences (NIGMS) repository (Camden, NJ).
8. H. S. Smith *et al.*, *J. Natl. Cancer Inst.* **78**, 611 (1987). According to the published karyotype, 600PE contains only one normal copy of chromosomes 1, 9, 11, 13, 16, and 17 and has five marker chromosomes: t(1q:13q), 1p-(p22), inv(11)(p15q13), t(9q:17q), and inv(1)(p36q21). FISH of 600PE interphase nuclei and metaphase chromosomes (*9*) showed two signals with 16p cosmid probes and one signal with 16q cosmids. The other 16p signal was located on the second marker chromosome, which indicates that this marker had been misclassified by conventional cytogenetic analysis and was actually a t(1q:16p).
9. M. Sakamoto, personal communication.
10. GMO5877 and GMO1142A come from the NIGMS repository (Camden, NJ).
11. K. W. Kinzker *et al.*, *Proc. Natl. Acad. Sci. U.S.A.* **83**, 1031 (1986).
12. C. Saint-Ruf *et al.*, *Genes Chrom. Cancer* **2**, 18 (1990); S. Bruderlein, K. van der Bosch, P. Schlag, M. Schwab, *ibid.*, p. 63.

13. We thank H. S. Smith and L. Chen for supplying 600PE DNA, M. Sakamoto for mapping the chromosome 16 deletion in 600PE cells, P. Kyrölä for technical assistance, and the Los Alamos National Laboratory for chromosome 16 cosmids. This work was funded by the Office of Health and Environmental Research, Department of Energy, under contract DE-AC-03-76SF00098, and NIH grants CA 45919, CA 44768, and CA 47537 as well as by Imagenetics Inc. (Naperville, IL). A.K. and O.-P.K. have received support from the Finnish Science Academy, Finnish and Pirkanmaa Cancer Societies, Lahtikari Foundation, and Pirkanmaa Cultural Foundation (Finland).

8 June 1992; accepted 15 September 1992

TECHNICAL COMMENTS

Mantle Plumes and Mantle Sources

Basalts from many ocean islands define elongate arrays in Sr-Nd-Pb isotopic space; these likely reflect the dominance of binary mixing of mantle sources in intraplate volcanism. S. R. Hart *et al.* (*1*) observe that when these arrays are projected onto a ternary diagram bounded by mantle endmembers DMM [depleted mid-ocean ridge basalt (MORB) mantle], HIMU (high U/Pb mantle), and EM1 (enriched mantle 1), they are subparallel and point toward a composition on the DMM-HIMU join. Hart *et al.* suggest this composition is associated with a high $^3He/^4He$ ratio (>30 R_A) and therefore cannot be a ubiquitous upper-mantle mixture of DMM and HIMU (both of which have $^3He/^4He$ < 9 R_A). They instead argue in favor of a new isotopic component, resident in a deep mantle "Focus Zone" (FOZO), which is characterized by a high $^3He/^4He$ ratio or which acquires helium with a high $^3He/^4He$ signature from the core.

There is an alternative interpretation of the He data. On the basis of binary isotope diagrams involving He, we (*2*) have suggested that the highest $^3He/^4He$ ratios are associated with intermediate $^{87}Sr/^{86}Sr$ and $^{143}Nd/^{144}Nd$ rather than with the highly depleted FOZO values. Mantle He-Sr-Nd-Pb systematics are consistent with five compositional endmembers—our finding of high $^3He/^4He$ Primitive Helium Mantle (PHEM) (*2*) and DMM-HIMU-EM1-EM2.

Combined He-Sr-Nd-Pb data are lacking for most ocean islands. However, many studies have demonstrated that ocean islands may be either "high ^3He" (all measured $^3He/^4He$ ratios ≥ MORB values) or "low ^3He" ($^3He/^4He$ ≤ MORB) (*3*). We know of no single ocean island that has $^3He/^4He$ ratios both greater and less than MORB (this also holds for most hot spot chains). Thus we can easily identify ocean islands that are tapping high $^3He/^4He$ material; if FOZO is characterized by a high $^3He/^4He$ ratio, then arrays trending toward it should be from high $^3He/^4He$ islands. We have replotted the mantle ternary (*1*) in Fig. 1 to indicate He affinities and the projection of the PHEM component into DMM-EM1-HIMU space. Many of the arrays tending toward FOZO are from low $^3He/^4He$ localities (Fig. 1), indicating that FOZO may not have a high $^3He/^4He$ ratio. We propose that some arrays mix to PHEM, and others to FOZO; isotopic relationships in DMM-HIMU-EM1-EM2-PHEM space are difficult to visualize in a ternary projection.

If FOZO does not have a high $^3He/^4He$ ratio, the need for a core or lower mantle helium source for FOZO is eliminated, and the component may be a DMM-HIMU mixture residing in the upper mantle. This has important implications for the origin and entrainment dynamics of mantle plumes. Additional studies of ocean islands, in which He is integrated with Sr-Nd-Pb, are required to accurately interpret $^3He/^4He$ ratios within the framework of the Sr-Nd-Pb mantle end-members.

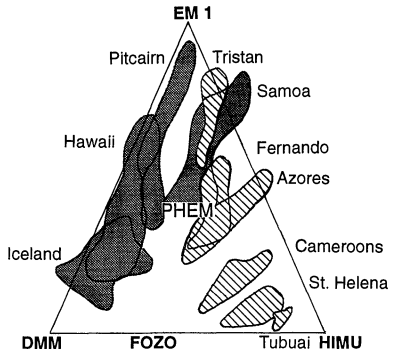

Fig. 1. Helium isotope affinity of some ocean island localities trending toward FOZO. Helium data are from standard sources [referred to in (*2, 3*)] and our unpublished results. Striped areas indicate low ^3He; solid areas indicate high ^3He.

K. A. Farley
Lamont-Doherty Geological Observatory, Palisades, NY 10964
H. Craig
Scripps Institution of Oceanography, La Jolla CA 92093

REFERENCES

1. S. R. Hart, E. H. Hauri, L. A. Oschmann, J. A. Whitehead, *Science* **256**, 517 (1992).
2. K. A. Farley, J. H. Natland, H. Craig, *Earth Planet. Sci. Lett.* 111, 183 (1992).
3. H. Craig, *EOS* 71, 1669 (1990); *Caltech Plume Symposium Abstract Volume 1* (Plumacy Press, California Institute of Technology, Pasadena, CA 1991).

1 June 1992; accepted 17 August 1992

Response: In our paper on evidence for lower mantle plume entrainment, we stressed the potential role that He isotopes could play in supporting or rejecting our theory. We noted the lack of published He data on many key islands, so we welcome the comment by Farley and Craig.

Unfortunately, data are needed for He *and* Sr, Nd, and Pb isotopes on the same samples, and figure 1 of the comment by Farley and Craig does not help in this respect. Pitcairn shows enormous variations

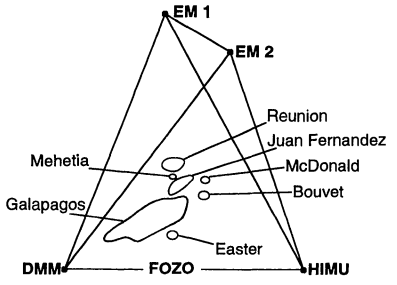

Fig. 1. Mantle tetrahedron from our report showing locations of additional high He 3/4 islands not shown in figure 1 of the comment by Farley and Craig. References for heavy isotope data may be found in (*3*); He data are from standard sources, Farley and Craig, and (*1*).